Electrocatalysis
https://doi.org/10.1007/s12678-022-00781-z

ORIGINAL RESEARCH

Electrocoagulation of Corrugated Box Industrial Effluents and Optimization by Response Surface Methodology

Belgin Karabacakoğlu[1] · **Filiz Tezakıl**[2]

Accepted: 30 September 2022
© The Author(s), under exclusive licence to Springer Science+Business Media, LLC, part of Springer Nature 2022

Abstract

The electrocoagulation method using stainless steel anodes was applied to a corrugated cardboard box manufacturing plant's wastewater with high COD content. The effects of current density, processing time and stirring speed on response functions were studied using the Response Surface Methodology (RSM). The removal efficiency of chemical oxygen demand (COD) and energy consumption were selected as response functions. The Central Composite Design (CCD) was chosen to explain the single and combined effects of independent variables on response functions. The COD concentration of the real industrial wastewater used in the experiments was 9130 mg L^{-1}. The maximum COD removal efficiency of 91.6% is obtained with 19.78 Wh g^{-1} energy consumption. Current density and treatment time were effective parameters for both COD removal and energy consumption. Optimization for maximum COD removal with minimum energy consumption showed 80.9% of COD removal with 6.7 Wh g^{-1} of energy consumption at 15 mA cm^{-2}, 700 rpm, and 28 min treatment time. The variables are optimized with a few experiments using the response surface method.

Keywords Electrocoagulation · Corrugated box wastewater · Response surface methodology · Central composite design · Optimization

Introduction

Paper, carton and corrugated board products with a total production of 2.1 million tons per year have become one of the leading sectors of the packaging industry in Turkey. These sectors account for 39% of the packaging industry, according to a report published in 2019 by the Ministry of Trade. Corrugated box packaging, which is a sustainable packaging material, is cheap and light; it has also a very high recovery ratio compared to all other packaging materials. As effect of the coronavirus pandemic, e-shopping has become widespread so the corrugated box needs and production increased. The production consists of two steps: adhering the corrugated cardboard and paper sheets with a special adhesive and performing the flexographic printing process on the cardboard. A high amount of water is used in the production of corrugated boxes, and therefore the amount of wastewater released at various stages is also high [1]. Generally, the wastewaters are a combination of starch, glue, and inks. Heavy metals are also present in the wastewater from colored inks. The most important environmental problem of corrugated cardboard wastewaters is that of having a high COD level. Because of the high COD and BOD content of the wastewater of corrugated box production facilities, it is difficult to treat. Therefore, it has significant impacts on environmental pollution, and the wastewater of this industry cannot discharge directly to the environment or sewage system. The first choice is to provide the discharge standard for the receiving environment with effective processing facilities. The second option is to discharge pretreated effluent to local industrial treatment facilities. Small or medium-sized plants prefer generally the second one from an economical point of view. In many countries, a wastewater treatment plant is located nearby an organized industrial zone to separate industrial effluents from domestic and sewage wastewaters for efficient treatment. A high-capacity wastewater treatment plant has been operated in Eskişehir Organized Industrial Zone (EOIZ) in Turkey since 2009. Their acceptance criteria for pollutants are determined concerning national registrations, and the COD discharge criteria of

✉ Belgin Karabacakoğlu
bkara@ogu.edu.tr

[1] Eskişehir Osmangazi University, 26480 Eskişehir, Turkey

[2] Turkish DemirDöküm Corp, Bozüyük Factory 11300, Turkey

Published online: 13 October 2022

corrugated box manufacturing effluents was 1200 mgL^{-1}. Therefore, the cardboard industry must provide this COD level with pretreatment using available treatment operations before discharge to a wastewater treatment plant.

Electrocoagulation (EC), which is an electrochemical treatment technique, can be successfully applied in the treatment of wastewater with different contents. Heavy metals such as Cr(VI) [2], arsenic [3] and organic pollutants such as dyes [4, 5] and pesticides [6] were removed from the model solution and wastewater by EC. The treatment tool of the electrocoagulation method is similar to chemical coagulation. The main difference between electrocoagulation and chemical coagulation is those electrode reactions are responsible for the production of coagulants necessary for treatment. Coagulants are produced by continuously releasing aluminum or iron ions of anodic metal by anodic oxidation in situ [7]. Simultaneously, hydroxide ions and hydrogen gas evolve at the cathode by water reduction. The hydroxide ions are used to create ferric, ferrous, and aluminum hydroxide which are efficient adsorbents. Hydrogen gas helps transport the formed flocs to the surface [8]. Contaminants may also be reduced or oxidized with cathode and anode, respectively. Furthermore, the smallest charged colloidal particles may be coagulated easily with the help of an electrical field. The main steps of EC are the evaluation of aluminum or iron ions by anodic dissolution; formation of coagulants in various forms in solution depending on the pH and ion types; adsorption of pollutants on coagulants and sedimentation or flocculation of coagulants adsorbed pollutants with the help of hydrogen gas [6]. Electrocoagulation is a cost-effective and rapid technique for the treatment of waters and wastewaters having different characteristics. Compared with traditional flocculation and coagulation, the EC has several advantages such as ease of operation, less retention time; not requiring pH control in most cases, rapid sedimentation of the flocculants, less sludge production, and lower capital cost. The effectiveness of the EC is influenced by numerous factors such as applied voltage, electrolyte conductivity, pH, electrolyte concentration, processing time, current density, electrode type and surface area. It is very useful to optimize some of these variables to increase the efficiency of the process and especially to reduce electrical energy consumption.

Response Surface Methodology (RSM) is a combination of mathematical and statistical methods for modeling and analysis of complex systems such as EC where a response of interest is affected by various variables [9]. RSM is used for designing experiments, modeling, examining the effect of several variables on a response, and determining the optimum conditions for desirable responses. Process modeling with RSM is performed in less time as it requires fewer experiments, and less experimentation means less resource use [10, 11]. Process variables for the treatment of wastewater such as slaughterhouse [12, 13], metal plating [14], paper mill [15], automobile [16], textile [17] and metal working [18] by electrocoagulation have been optimized using the response surface methodology. There are several studies in the literature that examine the treatment of real cardboard wastewater with electrocoagulation [1, 19, 20]. In one of these studies, optimization was made by response surface method for electrocoagulation/ozone hybrid method, but COD was selected as the only response and energy consumption was not optimized. However, energy consumption should also be optimized in terms of the applicability of electrocoagulation, an electrochemical treatment technique.

This study aims to optimize the process variables determined as current density, treatment time and stirring speed for minimum energy consumption and maximum COD removal by using the RSM method for the treatment of corrugated cardboard production wastewater with the electrocoagulation method.

Material and Method

Materials

The real wastewater was obtained from a factory producing corrugated cardboard packaging material in the industrial zone of Eskisehir city in Turkey. Starch and glue-free wastewater emerging from printing-painting operations were collected and stored in polyethylene bottles in a refrigerator at 4 °C until use. The suspended coarse particles in the wastewater were separated with the help of filter paper before experiments. Some parameters of wastewater were illustrated in Table 1.

Experimental Setup

Electrocoagulation experiment setup consists of DC power supply, magnetic stirrer and electrocoagulation reactor (Fig. 1). A 600 mL beaker was used as an EC reactor. Four plates made of AISI 304 stainless steel with dimensions of 9 cm × 6 cm × 0.2 cm were used as both anodes and cathodes. The total effective area of anodes immersed in wastewater was 139.2 cm^2. The distance between the electrodes

Table 1 Main characteristics of corrugated box wastewater

Parameter	Unit	Value
pH	-	7.2
Conductivity	mS cm^{-1}	2.08
COD	mg L^{-1}	9130
Total cyanide	mg L^{-1}	0.6
Cl^-	mg L^{-1}	990
Color	-	Reddish-brown

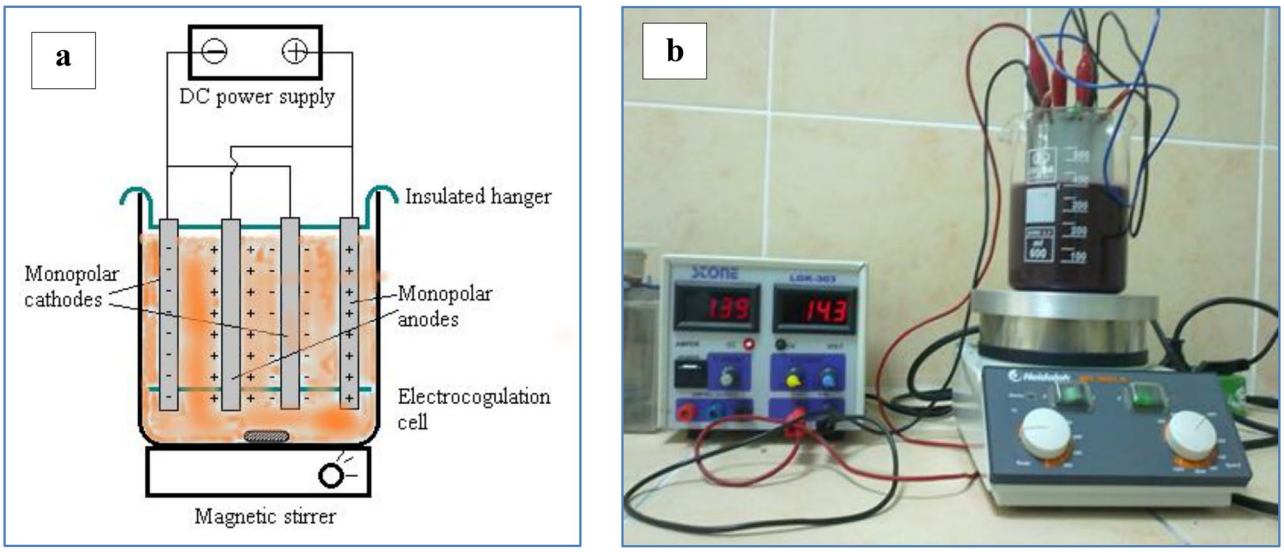

Fig. 1 Electrocoagulation set-up with monopolar parallel connection **a** schematic, **b** actual

was 1 cm, and an insulating hanger was used as an electrode separator to maintain the distance of the electrodes.

The anodes and cathodes were fixed two cm above the bottom of the cell to allow efficient mixing. Electrodes may be arranged as plate electrodes and connect to a power supply as monopolar or bipolar. Monopolar electrodes are connected parallel or serially to the power supply. For monopolar parallel electrode arrangement, electrodes connect separately to the DC power supply. This connection mode is the most efficient one because of the energy consumption [21]. For this reason, electrodes consisting of two anodes and two cathodes were connected as monopolar parallel to a DC power supply (0–20 V, 0–5 A). The wastewater was agitated by a magnetic stirrer.

Experimental Design and Data Analysis

In this study, the RSM via Design-Expert software (Stat-Ease Inc.) was used to develop a convenient, functional relationship between the selected responses and control variables. The experiments were designed according to Central Composite Design. The RSM was applied in the case of five stages [22]:

1. *The selection of variables that affect the aimed responses, and determination of the lower and upper levels of each variable:* The original pH and conductivity values of the wastewater were used for avoiding extra chemical usage. The current density, time, and stirring speed were chosen as parameters influencing the EC efficiency. The lower and upper limits of the variables were established by our preliminary experiments. COD removal efficiency (Y_1) and energy consumption (Y_2), which are important economical factors in electrochemical systems, were considered as the dependent factors (responses).
2. *The choice of the experimental design and studying the experimental runs is determined by the design model:* The second step of RSM is the selection of an experimental design model. For this purpose, a first-order and second-order model can be used. As shown in the literature, researchers have preferred generally the second-order symmetrical design such as three-level factorial design [23], central composite [24, 25], and Box-Behnken [20]. The selection of experimental points, the number of levels for variables, and the number of runs are different for each design model. CCD was selected as the design method in this study, and lower and upper levels of each variable were introduced to the software. All variables were studied in five levels as $-\alpha, -1, 0, +1, +\alpha$. α level of each variable depending on the number of variables (k) is determined by Eq. (1) [22]:

$$\propto = \sqrt[4]{2k} \tag{1}$$

α levels were calculated by the software. The levels to be used in the experimental design for the three factors determined as current density, treatment time and stirring speed are given in Table 2.

The total experiment number was determined by the software according to the following formula:

$$\text{Experiment number} = 2k + 2k + cp \tag{2}$$

Table 2 The variables and levels of the design model

Variable	Unit	Factors	Coded and actual variable				
			α-low	Low	Center	High	α-high
			−1.68	−1	0	+1	+1.68
Current density	mA cm^{-2}	X_1	6.6	10	15	20	23.5
Time	min	X_2	6.4	20	40	60	73.6
Stirring speed	rpm	X_3	164	300	500	700	836

where k is the number of variables, 2 k represents orthogonal points, 2 k represents axial points, cp corresponds to replicate the number of the central points [15, 22]. The CCD for three experimental variables included 20 experiments. Each experiment was run in the order given in Table 3 and only once. The number of repeats was 6 and provided an estimation of the experimental error, thus eliminating the repetition of other runs.

3. *The mathematical and statistical interpreting of the obtained experimental data through the fit of a polynomial function:* A total of 20 experiments were carried out under the conditions given in Table 3. The percentage of COD removal and energy consumption obtained for each experiment were entered into the program. Experimental data were analyzed using Design Expert and fitted to a second-order polynomial model, and then regression coefficients were obtained. The response (Y) of the process for determining experimental runs was used to evaluate the second-order polynomial equation as a function of selected variables (x) and their interactions according to the following equation [4, 26]:

$$Y = \beta_0 + \sum_{i=1}^{3} \beta_i x_i + \sum_{i=1}^{3} \beta_{ii} x_j^2 + \sum_{i=1}^{2} \sum_{j=i+1}^{3} \beta_{ij} x_i x_j \quad (3)$$

where $\beta 0$, βi, βii and βij are the regression coefficients for intercept, linear, quadratic, and interaction terms, respectively.

4. *The evaluation of the model fitness by ANOVA*: R^2 and R^2_{adj} regression coefficients were used to determine the appropriate polynomial model and statistical significance was checked with the *F*-test. The statistical significance of the models was justified through analysis

Table 3 Central composite design with actual values, experimental and predicted results

Run	*Variables*			*Responses*			
	Current density (mA cm^{-2})	Time (min)	Stirring speed (rpm)	COD Removal (%)		Energy consumption (Wh g^{-1})	
				Experimental	Predicted	Experimental	Predicted
1	15.0	40.0	164	75.0	76.6	8.74	8.77
2	10.0	20.0	300	67.6	65.0	2.69	2.60
3	20.0	60.0	300	79.4	81.2	21.51	24.88
4	15.0	40.0	836	82.3	82.9	7.92	8.75
5	15.0	40.0	500	82.8	83.1	7.92	11.30
6	15.0	6.4	500	69.1	70.3	1.63	2.68
7	10.0	20.0	700	71.2	68.4	2.59	1.91
8	15.0	40.0	500	83.1	83.1	8.99	11.26
9	10.0	60.0	700	74.4	72.6	7.02	10.21
10	20.0	60.0	700	83.6	85.1	21.06	23.77
11	15.0	40.0	500	83.4	83.1	7.86	11.22
12	15.0	40.0	500	84.4	83.1	12.56	11.09
13	15.0	73.6	500	73.3	74.1	21.06	23.84
14	6.6	40.0	500	57.3	63.6	3.63	5.85
15	23.4	40.0	500	91.6	87.4	19.81	20.11
16	20.0	20.0	300	80.1	80.8	9.45	9.25
17	10.0	60.0	300	70.7	67.1	9.49	12.01
18	15.0	40.0	500	82.6	83.1	11.81	11.33
19	20.0	20.0	700	80.1	82.7	9.49	10.01
20	15.0	40.0	500	82.4	83.1	12.30	11.36

of variance (ANOVA) for the quadratic model. For each response, three-dimensional surface graphs were created showing the binary interactions of the variables.

5. *Obtaining the optimum levels of each variable for the aimed levels of responses*: For numerical optimization, the desired goal of each factor and response from the menu of the program are chosen. Then, the program seeks the optimum points to maximize the desirability function [27]. The desired goal of each variable was chosen within the range introduced in Table 2. Different options are available for responses such as maximize, minimize, in range, none, and target.

Experimental Procedure and COD Analysis

The experiments were performed in the same order as given in Table 3. EC experiments were conducted in galvanostatic mode, and the constant current was adjusted to the required value. Four hundred mL of wastewater was used in each experiment. The conductivity of the wastewater was sufficiently high (Table 1), and any supporting electrolyte did not use. The wastewater was used without adjustment of pH. Therefore, additional chemical use was avoided. At the end of the experiment, the electrodes were removed, and the solution was filtered. Electrodes were rinsed with dilute HCl after each experiment. COD analysis was performed by the closed reflux colorimetric method. For analysis, 0.2 mL of sample was added to the Matriks® COD test kit (Turkey) and digested for 2 h at 148 °C in thermoreactor (Merck, TR320). Then, the tubes were cooled to room temperature, and the absorbance of the samples was read at 620 nm with a UV spectrophotometer (Thermo Scientific-Aquamate). The removal efficiency and energy consumption per COD removed were calculated using Eqs. (4) and (5), respectively:

$$\textit{COD Removal Efficiency}\ (\%) = \frac{C_0 - C}{C_0} 100 \tag{4}$$

$$\textit{Energy Consumption}\ \left(\mathrm{Whg}^{-1}\right) = \frac{\mathrm{UIt}}{\mathrm{V}\left(C_0 - C\right)} \tag{5}$$

where U, is the voltage (V); I, the current (A); t, the treatment time (h); V, the volume of wastewater (L); C_0 and C were the initial and present concentrations of the COD in solution (mg L^{-1}), respectively.

Results and Discussion

The most important parameter affecting the cost in terms of the applicability of electrochemical processes is energy consumption. Therefore, high removal efficiency and low energy consumption are required. In many EC studies with RSM, the removal efficiency was selected as a unique response [28, 29], and a few research deals with energy consumption [30–32]. The experiments were conducted at varying current density, time, and stirring speed determined by CCD to individual and combined effects of these variables on COD removal efficiency and energy consumption.

Fitting of Process Models and Statistical Analysis

Response surface methodology is a mathematical and statistical technique that is used to develop a convenient, functional relationship between selected responses (Y) and control variables (x). For the treatment of real cardboard industry wastewater by the electrocoagulation process, 20 experiments were conducted for 5 levels of each variable based on the central composite design. The experiments were conducted in the order given in Table 3 and measured and predicted responses of COD removal and energy consumption were listed in the same table.

The values of the predicted responses in terms of COD removal and energy consumption were calculated from Eqs. (6) and (7). The lowest COD removal 57.3% and the highest COD removal 91.6% were obtained in the range of the variables as shown in Table 3. The lowest and highest values of energy consumption were 2.68 kWh and 21.48 kWh per gram of removing COD, respectively.

After the responses were introduced by the Design Expert, the software seeks the most convenient model. The quality of the model and its power of prediction are related to the variance coefficient, R^2. A high R^2 value, close to 1, is desirable and has a reasonable agreement with adjusted R^2 [33].

The quadratic model was suggested for COD removal and energy consumption by the program. The R^2 value of 0.9077 has an acceptable agreement with the model adjusted R^2 value of 0.8245 for the COD removal equation. The R^2 values greater than 0.8 indicate that the regression models explained the process well [34]. The R^2 value and adjusted R^2 value for the energy consumption equation are higher and their values are close to each other. If the difference between R^2 and adjusted R^2 is less, the model fits the data well. ANOVA results of these quadratic models are presented in Table 4.

The main statistical parameters indicating the significance and acceptability of the model which used optimization of process variables by using RSM are the model Fisher variation ratio (*F*-value), the probability ratio (*p*-value), and adequate precision. As seen in Table 4, the model "F-values" of 10.92 and 26.92 implies that the models are significant for COD removal and energy consumption, respectively. The large "F values" indicated that most of the variation in

Table 4 ANOVA for COD removal and energy consumption

Factor	COD removal (%)[a]		Energy consumption (Wh g^{-1})[b]	
	F-value	*p*-value	*F*-value	*p*-value
Model	10.92	0.0004	24.24	< 0.0001
A-Current Density (mA cm^{-2})	64.15	< 0.0001	102.50	< 0.0001
B-Time (min)	1.78	0.2112	104.38	< 0.0001
C-Stirring Speed (rpm)	3.85	0.0783	0.43	0.5245
AB	0.14	0.7124	6.00	0.0343
AC	0.11	0.7463	0.18	0.6785
BC	0.22	0.6515	0.32	0.5866
A^2	9.93	0.0103	1.16	0.3066
B^2	20.08	0.0012	0.64	0.4438
C^2	2.04	0.1833	2.14	0.1744

[a] $R^2 = 0.9077$, $R^2_{adjust} = 0.8245$, *Adequate precision* = 10.31.

[b] $R^2 = 0.9562$, $R^2_{adjust} = 0.9167$, *Adequate precision* = 16.07.

the response can be explained by the regression equations. Table 4 shows also that the most significant term is the current density for two responses. In the case that *P*-value is lower than 0.05 implies that the model and terms are significant [28, 35]. Values greater than 0.1 indicate that the model terms are not significant. In this case, A, C, A^2, B^2 are significant model terms for COD removal, and A, B, AB, C^2 are a significant model in terms of energy consumption. The current density is a highly significant model term in both COD removal and energy consumption equations. Adequate precision compares the range of the predicted values at the design points to the mean prediction error. Its value greater than 4 is desirable and confirms the applicability of the model for navigation of the design space [29]. For the present study, adequate precisions were found as 10.31 and 16.54 for COD removal and energy consumption, respectively. Therefore, the quadratic model can be used to navigate design space [26].

Different models were fitted to the experimental data by the software to generate the regression equations. The quadratic model was chosen for further analysis of COD removal and energy consumption. The regression equations of Y_1 (COD removal percent) and Y_2 (energy consumption) with coded values obtained by Design-Expert are given in Eqs. (6) and (7), respectively.

$$Y_1 = 83.10 + 7.10A + 1.18B + 1.74C - 0.44AB - 0.39AC + 0.54BC - 2.73A^2 - 3.88B^2 - 1.25C^2 \quad (6)$$

$$Y_2 = 10.23 + 4.89A + 4.94B - 0.32C + 1.55AB + 0.27AC - 0.35BC + 0.51A^2 + 0.38B^2 - 0.69C^2 \quad (7)$$

The larger the coefficient in front of the variable, the more significant its effect on the response. Also, a sign of the coefficient indicates that the impact of the variable on response function is positive or negative. A positive sign in each variable represents a synergistic effect of the variables to response, while a negative sign indicates an antagonistic effect of the variables [27]. As shown in Eq. (6) current density (A), time (B), and stirring speed (C) have a positive effect on the COD removal; this means that COD removal increases with increasing all the variables examined. The most efficient variable is the current density on the COD removal and it affected approximately six times than time and stirring speed. The energy consumption is affected positively by current density and time, also their effects are near as seen in Eq. (7).

The suitability of the selected model to experimental data may also be confirmed by the diagnostic plots such as the normal plot of residuals and predicted versus actual [29]. The adequacies of the models suggested for R_1 and R_2 were interpreted by the residual graphs. These graphs are introduced by the software and they demonstrate the differences between predicted and observed response values [36]. Therefore, the graphs of normal probability and the graphs of residuals versus fitted values for COD removal and energy consumption were examined. As shown in Fig. 2, values of normality assumption are almost on a straight line.

Predicted values using the quadratic model given in Eqs. (6) and (7) and actual values obtained experimentally are compatible with each other as illustrated in Fig. 3 and a good correlation is available between them. Data points for both COD removal and energy consumption appear to be close to the diagonal lines.

Pareto Analysis

Pareto analysis can also be used to interpret the RSM results. The Pareto analysis calculates the contribution of each factor on the response, and the following equation is used [37]:

$$P_i = \frac{b_i^2}{\sum b_i^2} 100 \quad (8)$$

where b_i is the coefficient in front of the related factor given in Eqs. (6) and (7). Figure 4 shows the graphical results of Pareto analysis of COD removal and energy consumption equations with coded values. As seen in the Pareto graphic, the current density is the main parameter influencing the COD removal and its contribution is 91.9%. The current density and time have a similar contribution to energy consumption. The synergetic effect of current density and time is the highest for energy consumption at 92.5%.

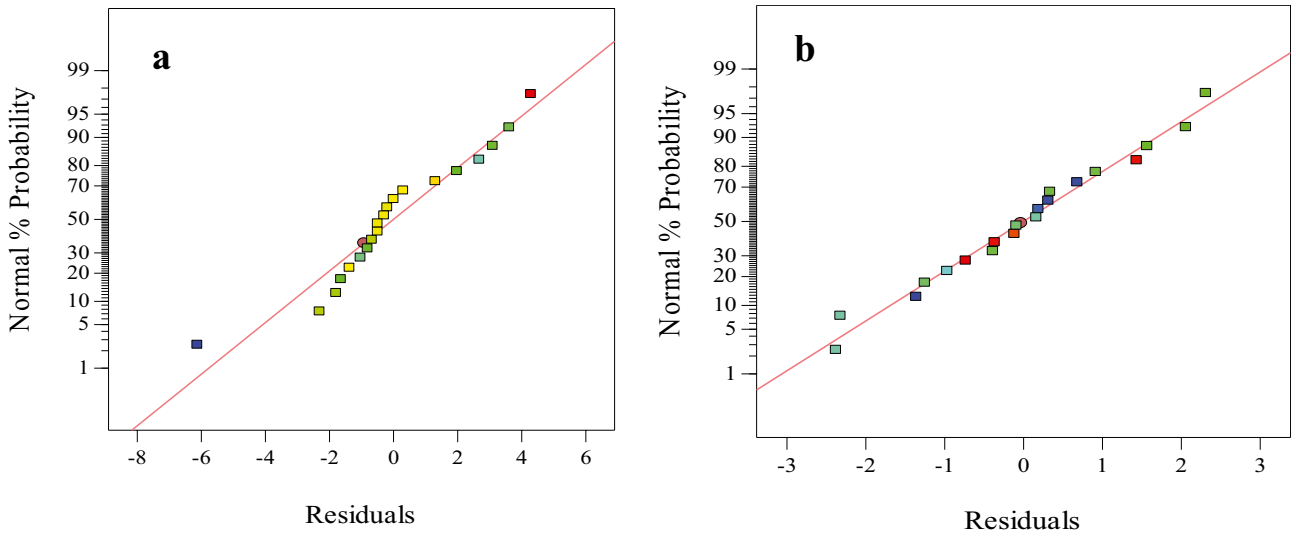

Fig. 2 Normal probability versus residuals plots for **a** COD removal and **b** energy consumption

Single and Combined Effects of Process Variables

The main advantage of response surface methodology is interpreting the interactions of process variables. The values of the response function obtained at varying current density, time, and stirring speed determined by CCD introduced the software. Three-dimensional curves of the response surfaces which were developed by the Design-Expert are shown in Figs. 5, 6, 7.

The interaction between current density (A) and time (B) on COD removal was performed by changing A from 10 to 20 $mAcm^{-2}$ under different B from 20 to 60 min, and the effects of current density and time of COD removal at 500 rpm stirring speed were illustrated in Fig. 5a. COD removal increased in increasing current density. Current density controls the generation amount and rate of coagulant and also the collision between the particles [29]. Colloidal particles were also destabilized more effectively at high current density [6]. As shown in Fig. 5, COD removal increased with an increase in current density due to the electrode reactions. According to Faraday's Law, the amount of dissolved anodic metal and hence coagulant dose is directly proportional to the applied current on an electrolytic cell at a certain time [38]. The main removal mechanism of EC is the adsorption of pollutants with the help of $Fe(OH)_2$ flocs. The increase in current density results in a higher amount of ferrous ions and hydroxides

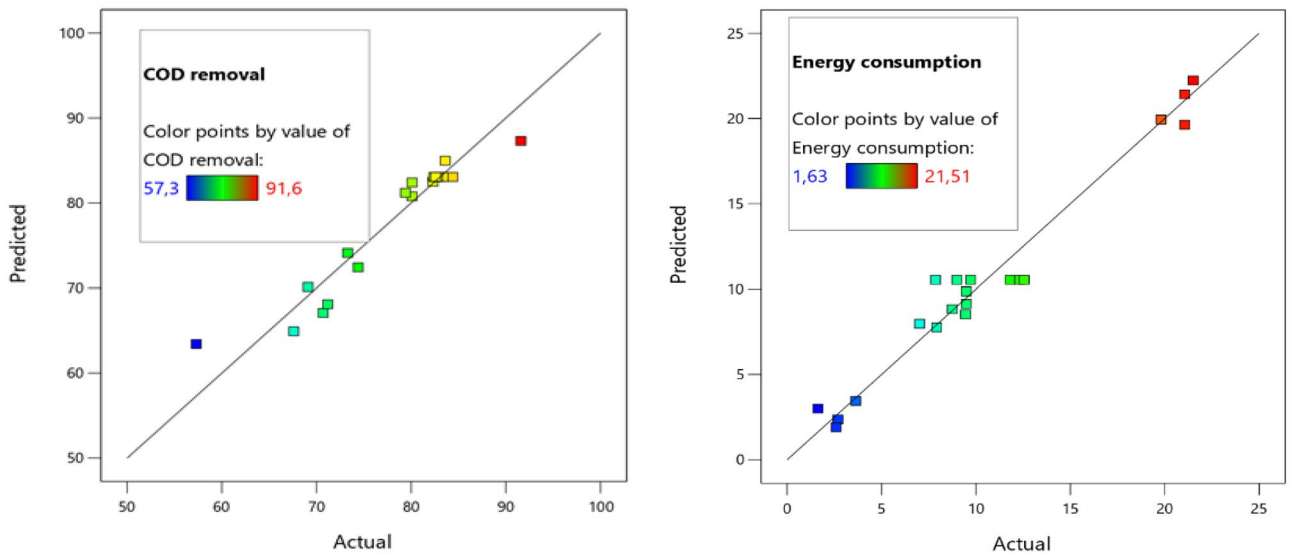

Fig. 3 Predicted from model equations versus actual (experimental) response plots for COD removal and energy consumption

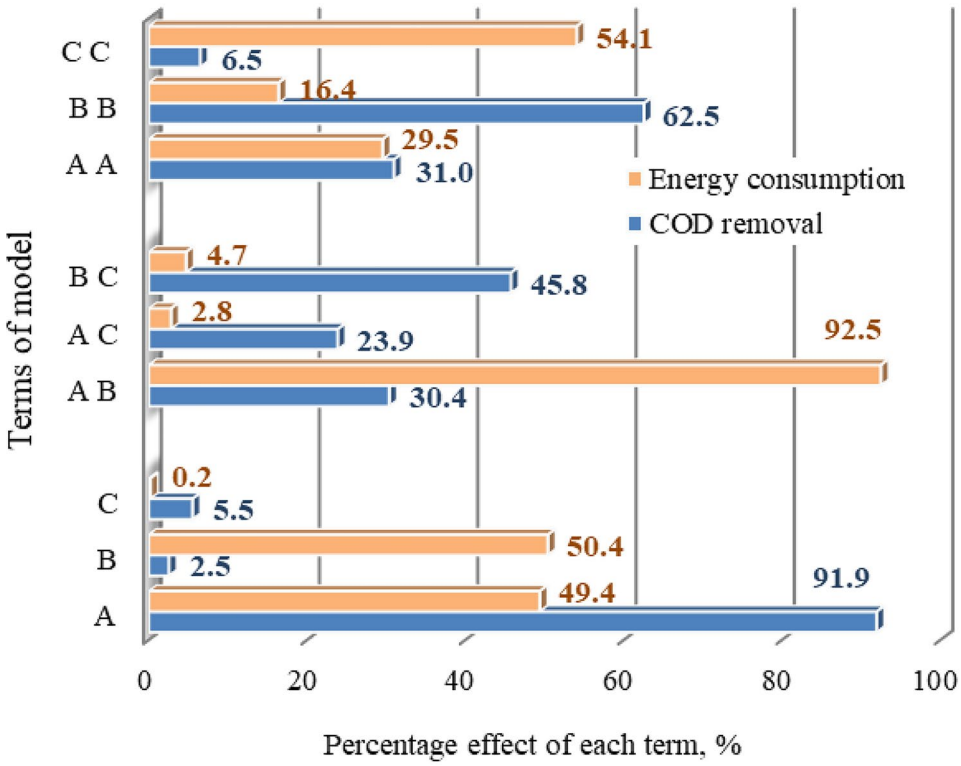

Fig. 4 Percentage effect of each term to responses obtained using the Pareto analysis (A: current density, mA cm^{-2}; B: time, min; C: stirring speed, rpm)

by the following reactions and therefore more ferrous hydroxide evaluates [39]:

$$\text{Anode}: \text{Fe} \rightarrow \text{Fe}^{2+} + 2e^{-} \quad (9)$$

$$\text{Cathode}: 2H_2O + 2e^{-} \rightarrow H_2(g) + 2OH^{-} \quad (10)$$

An increase in the current density increases the density of the bubbles liberated from electrodes and decreases the size of the bubble. Therefore, there was an improvement in the removal of COD and sludge production [40]. Although there was increase in the COD removal by increasing current density, its value must be limited due to ohmic heating which leads to increased solution temperature at high current density [29]. Ohmic heating was observed significantly at 23.5 mA cm^{-2} of current density. Energy consumption increased with the increase in time and current density as shown in Fig. 4b, and its effects were almost equal. It can be concluded from the

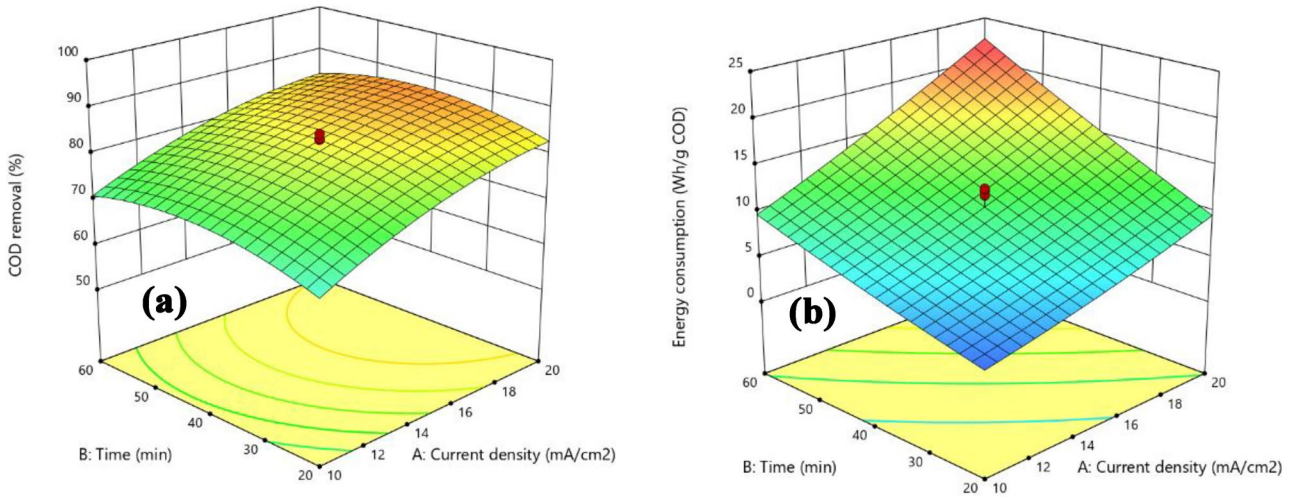

Fig. 5 3D surface graph of the combined effect of current density-time on **a** percentage of COD removal and **b** energy consumption (stirring speed: 500 rpm)

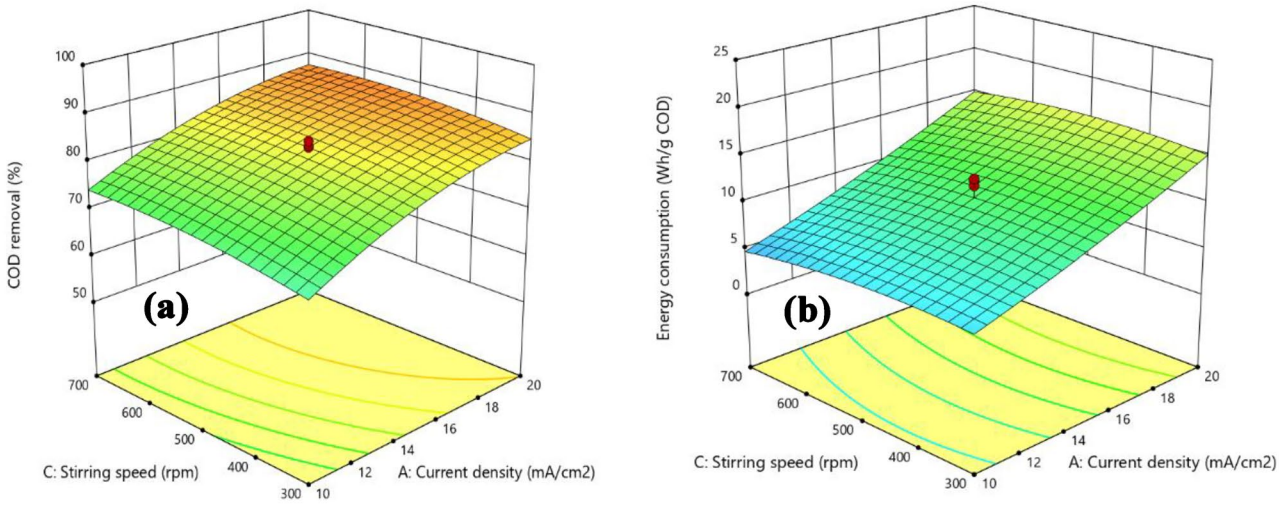

Fig. 6 3D surface graph for the combined effect of current density-stirring speed on **a** percentage of COD removal and **b** energy consumption (time: 40 min)

figures that higher COD removal and energy consumption are achieved at higher current density values.

Figure 6a and b illustrates the combined effect of mixing speed and voltage on the removal and energy consumption, respectively. The most important effect of the stirring speed is on the mass transfer. It can be seen from the figures that the COD removal slightly increased with the increase in the mixing speed. Similar results can be seen in the literature [41]. The increased stirring speed promotes turbulence, reduces the thickness of the diffusion layer at the electrode surface, and reduces cell resistance by facilitating the removal of gas bubbles that accumulate on the surface of the electrode [42]. Another function of the stirring is to distribute the iron-based coagulants effectively throughout the reaction. The stirring of the electrolyte ensures that the temperature and pH values are homogenous throughout the reactor. However, high stirring rates may break the flocks formed in the reactor and form small flocks which are hard to remove from water [43, 44].

Figure 7a and b was used to explain the combined effect of stirring speed (300–700 rpm) and time (20–60 min) on removal efficiencies of color and COD, keeping the third parameter at center value as 15 mA cm^{-2}. As seen from these figures, to reach the maximum COD removal, the average treatment time (44 min) and the stirring speed over 500 rpm are required, the low treatment period results in lower energy

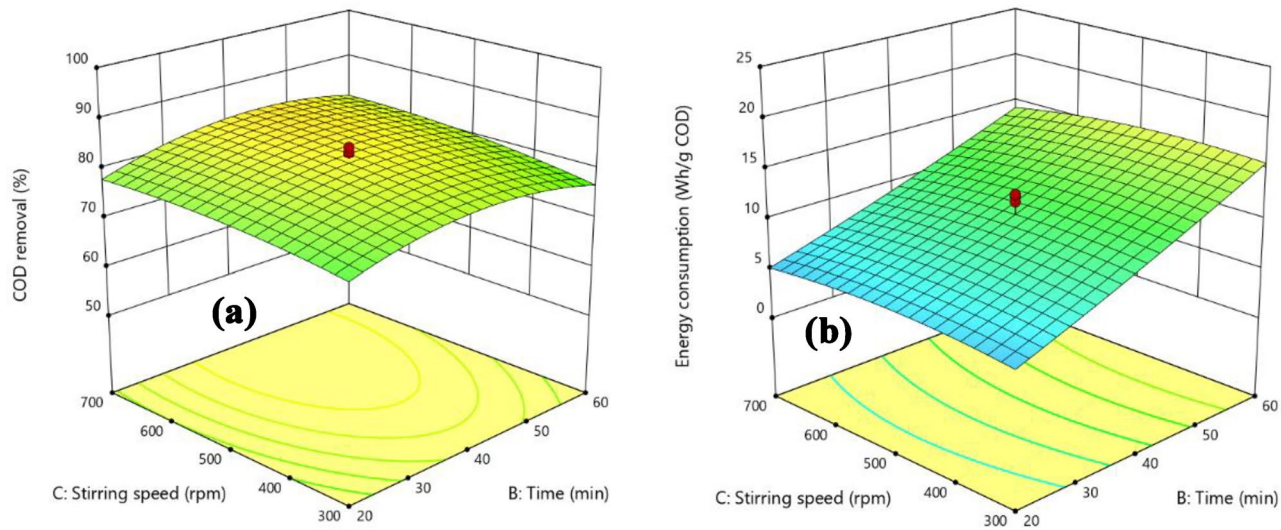

Fig. 7 3D surface graph of the combined effect of time-stirring speed on **a** percentage of COD removal and **b** energy consumption (current density: 15 mA cm^{-2})

consumption. It is also observed that stirring speed has no significant impact on energy consumption. Also, higher treatment time results in higher sludge formation. It can be noted that the COD removal increased up to 75.3% and 78.03%, respectively, upon increasing the stirring speed from 300 to 700 rpm at 15 mA cm^{-2} current density. The treatment time affected the energy consumption much more, as the energy consumption for a current density of 15 mA cm^{-2} and a mixing speed of 300 rpm increased from 4.95 to 14.19 Wh g^{-1} as the time increased from 20 to 60 min.

Optimization of Experimental Variables

The optimization of process variables was realized by the Design-Expert software. The most important advantage of RSM is the ability to optimize multiresponse. For numerical optimization, the desired goal of each factor and response from the menu of the program are chosen. Then, the program seeks the optimum points to maximize the desirability function [27]. The desired goal of each variable (current density, time, and stirring speed) was chosen within the range introduced in the Table. The COD removal was defined as maximum to achieve the highest efficiency while the energy consumption was defined as a minimum from the economical point of view. The software searched the optimum values of variables to ensure the responses for common desirability and offered 8 solutions. The solutions were very close to each other. The optimized conditions were obtained as 15 mA cm^{-2} current density, 700 rpm stirring speed, and 28 min treatment time with the desirability of 0.72. At these optimum conditions, 80.9% of COD removal and 6.7 Wh g^{-1} of energy consumption were foreseen by the program optimization. Because 80.9% of COD removal does not satisfy the national limits of discharge to a sewage system, the optimization criteria were changed. Energy consumption was defined within the range, while the desired goal of variables and COD removal remained the same. In these conditions, software was the current density of 20 mA cm^{-2}, stirring speed of 600 rpm and treatment time of 42 min were obtained optimized values of independent variables with the COD removal of 88% and energy consumption per COD removed of 16 Wh g^{-1}. The desirability is 0.89. High removal rates of the COD resulted in high energy consumption. Similar results were obtained by Taheri et al. [45]. In the experiment carried out under these conditions, 88.1% COD removal was obtained.

Conclusions

The efficiency of the EC process with stainless steel anodes for COD removal from industrial wastewater was studied, and the impact of process variables such as current density, treatment time, and stirring speed on removal percent of COD and energy consumption by using RSM with Central Composite Design. The analysis of the experimental results by ANOVA indicated that RSM was a practical and appropriate method to optimize the process variables. The maximum COD removal efficiency of 91.6% with energy consumption of 19.78 Wh g^{-1} COD was obtained under the following conditions: 23.4 mA cm^{-2} of current density, 40 min of treatment time, and 500 rpm of stirring speed. To achieve high removal efficiencies of COD, applied current density should be increased, but increasing the current density increases the energy consumption. From this point of view, the optimized levels of factors evaluated by the software were current density of 20 mA cm^{-2}, treatment time of 42 min, stirring speed of 600 rpm with the COD removal of 88%, and energy consumption of 16 Wh g^{-1} COD. Under these conditions, it will be possible to lower the COD concentration of wastewater (9130 mg L^{-1}) to the COD discharge limit of 1200 mg L^{-1}. Moreover, pH adjustment was not necessary, and we studied the original pH of the real wastewater in all experiments. The theory of EC is also based on the dissolving of the anodes, therefore it needs to be replaced in a specific time interval. Stainless steel electrodes can be used longer than iron and aluminum electrodes. At the end of the experiments, it was observed that there was only pinhole corrosion on the surfaces of the anodes.

Declarations

Conflict of interest The authors declare no competing interests.

References

1. S. Bellebia, S. Kacha, A.Z. Bouyakoub, Z. Derriche, Environ. Prog. Sustain. Energy **31**, 361 (2012)
2. H. Xu, Z. Yang, G. Zeng, Y. Luo, J. Huang, L. Wang, P. Song, X. Mo, Chem. Eng. J. **239**, 132 (2014)
3. A.Y. Goren, M. Kobya, Chemosphere **263**, (2021)
4. A.S. Assemian, K.E. Kouassi, P. Drogui, K. Adouby, D. Boa, Water Air Soil Pollut. **229**, (2018)
5. M. Taheri, Clean. Chem. Eng. **2**, 100007 (2022)
6. M. Behloul, H. Grib, N. Drouiche, N. Abdi, H. Lounici, N. Mameri, Sep. Sci. Technol. **48**, 664 (2013)
7. M. Kobya, R.D.C. Soltani, P.I. Omwene, A. Khataee, Environ. Technol. Innov. **17**, (2020)
8. G. Chen, Sep. Purif. Technol. **38**, 11 (2004)
9. M. Kumari, S.K. Gupta, Sci Rep **9**, 18339 (2019)
10. M.S. Bhatti, A.S. Reddy, A.K. Thukral, J Hazard Mater **172**, 839 (2009)
11. M. Saleh, R. Yildirim, Z. Isik, A. Karagunduz, B. Keskinler, N. Dizge, Water Sci. Technol. **84**, 1245 (2021)
12. A.S.K. Al-Saidi, N.N.S. Al Rashidi, M.G. Devi, V.M. Joy, Appl. Water Sci. **11**, (2021)
13. M. Tanyol, S. Tevkur, Desalin. Water Treat. **223**, 227 (2021)
14. M.K. Oden, Fresenius Environ. Bull. **28**, 9049 (2019)

15. N. Pandey, C. Thakur, Process Integr. Optim. Sustain. **4**, 343 (2020)
16. T. Chandrakant, IOP Conf. Ser. Earth Environ. Sci. p. 012017 (2020)
17. S. Hanumanthappa, M. Shivaswamy, S. Mahesh, Desalin. Water Treat. **146**, 85 (2019)
18. S.Y. Guvenc, Y. Okut, M. Ozak, B. Haktanir, M.S. Bilgili, Water Sci Technol **75**, 833 (2017)
19. E. Gengec, Ecotoxicol Env. Saf **145**, 184 (2017)
20. M. Mehralian, M. Khashij, A. Dalvand, Env. Sci Pollut Res Int **28**, 45041 (2021)
21. E. Gengec, M. Kobya, E. Demirbas, A. Akyol, K. Oktor, Desalination **286**, 200 (2012)
22. M.A. Bezerra, R.E. Santelli, E.P. Oliveira, L.S. Villar, L.A. Escaleira, Talanta **76**, 965 (2008)
23. K. Missaoui, W. Bouguerra, C. Hannachi, B. Hamrouni, J. Water Resour. Prot. **05**, 867 (2013)
24. E. Gengec, U. Ozdemir, B. Ozbay, I. Ozbay, S. Veli, Water, Air, Soil Pollut. **224**, (2013)
25. A.R. Shah, H. Tahir, S. Sadi, Pakistan J. Anal. Environ. Chem. **20**, 115 (2019)
26. B. Mondal, V.C. Srivastava, I.D. Mall, J. Env, Sci Heal. A Tox Hazard Subst Env. Eng **47**, 2040 (2012)
27. M.D. Pavlović, A.V Buntić, K.R. Mihajlovski, S.S. Šiler-Marinković, D.G. Antonović, Ž. Radovanović, S.I. Dimitrijević-Branković, J. Taiwan Inst. Chem. Eng. (2014)
28. A.R. Amani-Ghadim, S. Aber, A. Olad, H. Ashassi-Sorkhabi, Chem. Eng. Process. Process Intensif. **64**, 68 (2013)
29. M.H. Isa, E.H. Ezechi, Z. Ahmed, S.F. Magram, S.R. Kutty, Water Res **51**, 113 (2014)
30. A.I. Adeogun, P.B. Bhagawati, C.B. Shivayogimath, J Env. Manag. **281**, (2021)
31. M.S. Bhatti, D. Kapoor, R.K. Kalia, A.S. Reddy, A.K. Thukral, Desalination **274**, 74 (2011)
32. S. Abbasi, M. Mirghorayshi, S. Zinadini, A.A. Zinatizadeh, Process Saf. Environ. Prot. **134**, 323 (2020)
33. M. Kobya, E. Demirbas, M. Bayramoglu, M.T. Sensoy, Water, Air. Soil Pollut. **215**, 399 (2010)
34. E. Yuliwati, A.F. Ismail, W.J. Lau, B.C. Ng, A. Mataram, M.A. Kassim, Desalination **287**, 350 (2012)
35. A.R. Khataee, M. Zarei, L. Moradkhannejhad, Desalination **258**, 112 (2010)
36. M. Behbahani, M.R.A. Moghaddam, M. Arami, Desalination **271**, 209 (2011)
37. G. Varank, S.Y. Guvenc, K. Dincer, A. Demir, Int. J. Environ. Res. **14**, 439 (2020)
38. T. Olmez-Hanci, Z. Kartal, I. Arslan-Alaton, J. Environ. Manage. **99**, 44 (2012)
39. K. Gautam, R.K. Verma, S. Kamsonlian, S. Kumar, Chem. Prod. Process Model. **16**, 129 (2021)
40. R. Katal, H. Pahlavanzadeh, Desalination **265**, 199 (2011)
41. S. Camcioglu, B. Ozyurt, H. Hapoglu, Process Saf. Environ. Prot. **111**, 300 (2017)
42. R. Sridhar, V. Sivakumar, V.P. Immanuel, J.P. Maran, Environ. Prog. Sustain. Energy **31**, 558 (2012)
43. S. Bayar, Y.S. Yildiz, A.E. Yilmaz, S. Irdemez, Desalination **280**, 103 (2011)
44. J.B. Parsa, H.R. Vahidian, A.R. Soleymani, M. Abbasi, Desalination **278**, 295 (2011)
45. M. Taheri, M.R. Alavi Moghaddam, M. Arami, J Env. Manag. **128**, 798 (2013)

Publisher's Note Springer Nature remains neutral with regard to jurisdictional claims in published maps and institutional affiliations.

Springer Nature or its licensor holds exclusive rights to this article under a publishing agreement with the author(s) or other rightsholder(s); author self-archiving of the accepted manuscript version of this article is solely governed by the terms of such publishing agreement and applicable law.